Current Research in Food Science 5 (2022) 1395–1402

Contents lists available at ScienceDirect

Current Research in Food Science

journal homepage: www.sciencedirect.com/journal/current-research-in-food-science

A monoclonal antibody-based time-resolved fluorescence microsphere lateral flow immunoassay for paclobutrazol detection

Yongjian Cheng, Bo Xie, Yifan Liang, Xinmei Liu, Haojie Chen, Jiadong Li, Hongtao Lei, Zhili Xiao *

Guangdong Provincial Key Laboratory of Food Quality and Safety, College of Food Science, South China Agricultural University, Guangzhou, 510642, China

ARTICLE INFO

Handling Editor: Dr. Quancai Sun

Keywords:
Paclobutrazol
Monoclonal antibody
Time-resolved fluorescence microsphere
Lateral flow immunoassay

ABSTRACT

Paclobutrazol (PBZ) is a plant growth inhibitor and fungicide, but it is also carcinogenic and teratogenic, and has potential harm to human health. In this study, two PBZ haptens (PBZ-1, PBZ-2) were synthesized and conjugated with carrier proteins to get artificial antigens. A highly specific monoclonal antibody (mAb) against PBZ was prepared. The antibody subtype was IgG_1 and the concentration was 11.03 mg/mL. A sensitive and rapid time-resolved fluorescence microsphere lateral flow immunoassay (TRFMs-LFIA) was established based on the mAb. The activated pH, the mAbs diluents, the mAb reacting concentration and the probe amount were optimized. The visual limit of detection (vLOD) and quantitative limit of detection (qLOD) of the TRFMs-LFIA for PBZ were 50 and 1.72 ng/mL respectively, and the 50% inhibiting concentration (IC_{50}) was 9.38 ng/mL. The pretreatment procedures are simple and rapid, and the detection time of TRFMs-LFIA strip is 6 min. Qualitative and quantitative analysis of PBZ could be achieved under a UV light or with a portable fluorescence immunoassay analyzer. The average recovery rates ranged from 96.2% to 111.9% and the corresponding coefficients of variation (CV) were 4.0%–11.2% in spiked wheat and rice samples. Twenty real wheat and rice samples were measured by the TRFMs-LFIA and compared with Ultra-performance liquid chromatography/tandem mass spectrometry (UPLC-MS/MS). The measured values showed a good accordance. These results indicated that the proposed assay will provide a novel effective strategy for on-site detection of PBZ.

1. Introduction

Paclobutrazol (PBZ) is a plant growth inhibitor and fungicide with high efficiency and low toxicity (Hua et al., 2014; Peng et al., 2014; Shah et al., 2017). It is widely used in rice, wheat and other economic crops (Jiang et al., 2019; Cao et al., 2014). However, excessive use will lead to a large amount of PBZ residue in the soil. Studies have shown that PBZ can enter human body through the food chain and may cause harm to human reproductive system (Wang, 2016). At the same time, after being degraded by microorganisms, the residual PBZ in the environment can also generate some intermediate products with carcinogenic and teratogenic effect (Liu et al., 2015, 2016; Kishore et al., 2015; Wu et al., 2015). In addition, due to its slow degradation rate and long half-life, PBZ cannot be eliminated via routine treatment processes, which will lead to the decline of soil fertility and quality (Ouyang et al., 2020; Gonçalves et al., 2009; Cregg and Ellison-Smith, 2020; Guo et al., 2021). Considering the hazards of PBZ, many organizations and countries have set up the maximum residue limits (MRLs) of PBZ. In China, the MRL for PBZ in cereals was 0.5 mg/kg (GB 2763-2021). The European Union (EU) has stipulated that the maximum residue must not exceed 0.02 mg/kg in fruits (Authority E F S, 2007). Therefore, it is necessary to establish effective detection methods for PBZ residue in agri-products as well as around environment.

At present, there are two main types of detection methods for PBZ. Instrumental methods such as ultra-high performance liquid chromatography tandem mass spectrometry (UPLC-MS/MS) (Liu et al., 2015), Liquid chromatography-electrospray tandem mass spectrometry (LC-ESI-MS-MS) (Sancho et al., 2003), has good sensitivity and accuracy, but they require expensive equipment, complicated sample preparation procedures and professional operators. Alternatively, due to its high sensitivity, high specificity and simple operation, immunoassay has been widely used in pesticides detection. The immunological technologies for PBZ detection were listed in Table 1. An indirect competitive enzyme-linked immunosorbent assay (icELISA) reported by Cao et al.

* Corresponding author.
E-mail address: scau_xzl@163.com (Z. Xiao).

https://doi.org/10.1016/j.crfs.2022.08.017
Received 21 April 2022; Received in revised form 4 July 2022; Accepted 22 August 2022
Available online 27 August 2022

(2014) is quite sensitive, with an IC_{50} of 8.7 ng/mL. Liu et al. (2016) developed a time-resolved fluorescence immunoassay (TRFIA) using Eu^{3+}-labeled goat-anti-rabbit antibody instead of traditional horseradish peroxidase labeled secondary antibody for detection of PBZ residues in environmental water and soil samples, with IC_{50} of 1.09 ng/mL. Although the above methods have high throughput and sensitivity, they still require a long incubation time and multiple steps which hinder their application in field detection. For example, the detection time of icELISA established by Cao et al. (2014) takes 60 min, and the TRFIA established by Liu et al. (2016) takes 125 min. In order to achieve the real-time and on-site detection requirements, it is in demand to develop more simple and rapid screening strategies for PBZ.

Lateral flow immunoassay (LFIA) is a rapid detection method with the advantages of simplicity, rapidity, and visuality. It is suitable for real-time and on-site detection and has become a popular research topic in recent years (Anfossi et al., 2013; Shan et al., 2015). It works on the principle of specific recognition between immunoprobe and coating antibody/antigen immobilized on the nitrocellulose membrane under the action of capillary. The generated signal is proportional to the amount of the analyte (Di Nardo et al., 2021; Posthuma-Trumpie Geertruida et al., 2009). Signal probe types and characteristics can significantly impact the sensitivity of the method. Colloidal gold is commonly applied signal probe, but its disadvantages of unstable signal and insufficient sensitivity came out gradually in recent years (Liu et al., 2015). In order to improve stability and sensitivity, some researchers have prepared new signal probes including quantum dots (Mihaela et al., 2018), upconversion nanoparticles (Liu et al., 2014), time-resolved fluorescent microsphere (TRFM) (Sun et al., 2021; Wu et al., 2021) and magnetic nanobeads (Xu et al., 2009), etc. TRFM takes rare earth ions with long half-lives and long fluorescence lifetimes as signal probes. Due to the large Stokes shift (>150 nm), the fluorescence lifetime of TRFM is 5–6 longer than that of the background material (Sun et al., 2021). Therefore, the interference of various non-specific fluorescence can be eliminated by delaying the measurement time (Wu et al., 2021). Besides, TRFM is a special functional microsphere, and each contains thousands of fluorescent molecules. This could greatly improve the fluorescence labeling efficiency and effectively raise the assay sensitivity (Li et al., 2021; Juntunen et al., 2012). In addition, the outer layer of the TRFM is combined with appropriate functional groups such as carboxyl for covalent coupling to antibodies and enhance the labeling stability (Kokko et al., 2007; Song et al., 2014). From the foregoing, compared with traditional and widely used signal probe such as colloidal gold, LFIA based on TRFMs can reduce background fluorescence interference, and improve labeling efficiency and stability, thereby significantly increase assay sensitivity. So far, no LFIA for PBZ detection has been reported.

In this study, a specific anti-PBZ mAb was prepared. Then, TRFMs were coupled with the mAb to prepare immunoprobes. A LFIA with high sensitivity for rapid qualitative and quantitative detection of PBZ residues was developed. The accuracy of the developed TRFMs-LFIA was validated by UPLC-MS/MS.

2. Materials and methods

2.1. Reagents

PBZ, ovalbumin (OVA), bovine serum albumin (BSA), keyhole limpet hemocyanin (KLH), thyroglobulin (THY), 2-(N-morpholino) ethane sulfonic acid (MES), polyethylene glycol (PEG) 2000, goat anti-mouse Immunoglobulin G (IgG), complete and incomplete Freund's adjuvants were bought from Sigma-Aldrich Chemical Co. (St. Louis, MO, USA). Hypoxanthine-aminopterin-thymidine (HAT), hypoxanthine-thymidine (HT), RPMI-1640 culture media, fetal bovine serum (FBS), pierce rapid isotyping kits-mouse were purchased from Thermo Fisher Scientific Co., Ltd. (Waltham, MA, USA). N-hydroxysuccinimide (NHS, 99%), N-(3-dimethylaminopropyl)-N′-ethylcarbodiimide hydrochloride (EDC, 99%), N,N-dicyclohexylcarbodiimide (DCC, 99%), succinic anhydride, N,N-dimethylformamide (DMF) were purchased from Aladdin Chemistry Co., Ltd. (Shanghai, China). Time-resolved fluorescence microsphere (TRFM), europium chelates (365/610), 0.2 μm, 1% (w/v) solids suspension were purchased from Bangs Laboratories, Inc. (Indiana, USA). The standards of PBZ (≥98%), tebuconazole (≥98%), triadimefon (≥98%), hexaconazole (≥98%), diniconazole (≥98%), triadimenol (≥98%), uniconazole (≥98%) were purchased from Sinopharm Group Chemical Reagent Co., Ltd. (Shanghai, China). All organic solvents and chemicals used were of analytical grade.

2.2. Instruments and materials

Cell culture plates were purchased from Corning Incorporated (New York, USA). The absorbent pad (CH37K), PVC backing plate (SMA31-40) and sample pads (RB65) were purchased from Shanghai Liangxin Co., Ltd. (Shanghai, China). The Nitrocellulose (NC) membranes (Sartorius, UniSart CN95) were purchased by Sartorius Stedim Biotech GmbH (Goettingen, Germany).

The Lynx 4000 centrifuge was obtained from Thermo Fisher Scientific Co., Ltd. (Waltham, MA, USA). The BioDot-XYZ3060 Dispensing Platform was purchased from BioDot Inc. (Irvine, CA, USA). The strip cutter ZQ 2000 were purchased from Shanghai kinbio Tech. Co., Ltd. (Shanghai, China). The NanoDrop 2000c UV–vis spectrophotometer was provided by Thermo Fisher Scientific Co. (Waltham, Massachusetts, USA). An FIC-Q1 multifunctional fluorescence reader was purchased from Fenghang technology Co., Ltd. (Hangzhou, China). The Zetasizer Nano ZS90 used for measurement of size and charge of nanoparticles was supplied by Malvern Panalytical (Malvern, UK). Liquid chromatography triple-quadrupole mass spectrometry was carried out using a 1200 series LC system (Agilent Technologies, Santa Clara, USA) and nuclear magnetic resonance (NMR) spectrometry was recorded with DRX-600 spectrometer (Bruker, Flanders, Switzerland).

Female Balb/c mice were purchased from Guangdong Medical Laboratory Animal Center (Foshan, China). Rice and wheat samples were all purchased from a supermarket in Guangzhou, China.

2.3. Synthesis of antigens

According to the reported literatures with some modifications (Cao et al., 2014; Ouyang et al., 2020), two haptens termed PBZ-1 and PBZ-2 were synthesized, as shown in Fig. S1. PBZ-1 and PBZ-2 were conjugated

Table 1
Immunoassays for detecting of PBZ.

Immunoassay	IC_{50} (ng/mL)	LOD (ng/mL)	Antibody	Samples	Detection time (min)	References
icELISA	8.7	2.0	monoclonal antibody (mAb)	Wheat	60	Cao et al. (2014)
icELISA	11.6	0.9	mAb	Soil	60	Jin (2019)
icELISA	13.26	1.27	polyclonal antibody (pAb)	Fruits	85	Ouyang et al. (2020)
icELISA	21.35	0.43	pAb	Water and soil	75	Wang (2016)
TRFIA	1.09	0.069	pAb	Water and soil	125	Liu et al. (2016)

to carrier proteins (OVA, BSA, KLH, THY) respectively via activated ester method. An active ester intermediate was formed by mixing 10 μmol PBZ-1 or PBZ-2 with 12 μmol DCC and 12 μmol NHS (in 1 mL DMF) before stirring overnight at 4 °C. Carrier proteins were each dissolved with 3 mL of CBS buffer (0.01 M, pH 9.6), and the mole ration of carrier protein to antigen was 1:60 (BSA and OVA) or 1:200 (KLH and THY). The activated intermediate droplets were distributed in the carrier protein solutions, and the conjugation mixtures were reacted overnight at 4 °C, and then dialyzed against PBS for 3 d. The conjugates (PBZ-1-OVA, PBZ-1-BSA, PBZ-1-KLH, PBZ-1-THY, PBZ-2-BSA) were characterized by UV–vis spectroscopy.

2.4. Preparation of anti-PBZ mAb

Each six-week-old female Balb/c mouse was immunized subcutaneously with 100 μL of immunogen (PBZ-1-OVA, or PBZ-1-KLH, or PBZ-1-THY) and Freund's adjuvant mixture biweekly intervals. One week after the third booster injection, the antisera from mice tail were collected for sensitivity test by icELISA. The mouse that showed the best performance was used for cell fusion.

Cell fusion procedures were performed as follows (Galfre et al., 1981): the mice splenocytes were collected and fused with 1/5 amount of SP2/0 cells under the action of PEG2000. The fusion cells were distributed in 24-well plates and cultured in HAT selective medium. 10 d later, the supernatants were detected by icELISA using 1 μg/mL of coating antigen (PBZ-1-BSA or PBZ-2-BSA). The positive hybridoma cells were sub-cloned by limiting dilution. The hybridoma that secreting anti-PBZ mAb was inoculated into the abdominal cavity of Balb/C mice, and the ascites generated were purified by Protein G affinity chromatography to get mAb. The purity and content of the mAb were identified by SDS-PAGE gel electrophoresis and measured by NanoDrop 2000C spectrophotometer respectively. MAb isotyping kit and icELISA were used to detect antibody subtypes and evaluate the antibody performance, respectively.

2.5. Preparation of TRFMs immunoprobes

The TRFMs immunoprobes were prepared by activating the carboxyl on the TRFMs and coupling them with the mAbs (Fig. 1a). Initially, 10 μL of TRFMs (1%, w/v) was mixed with 1 mL of activation buffer (MES, 0.05 M), and dispersed with an ultrasonic device. After centrifuged at 12,000 rpm for 15 min, the precipitate was redissolved with 1 mL of MES buffer. Next 15 μg of EDC and 20 μg of NHS were dissolved in the solution, followed by gently shaken for 15 min at 25 °C. Then the mixture was centrifuged at 12,000 rpm for 15 min. The sediment was resuspended with 1 mL coupling buffer (20 mM Boric acid buffer, pH 8.0).

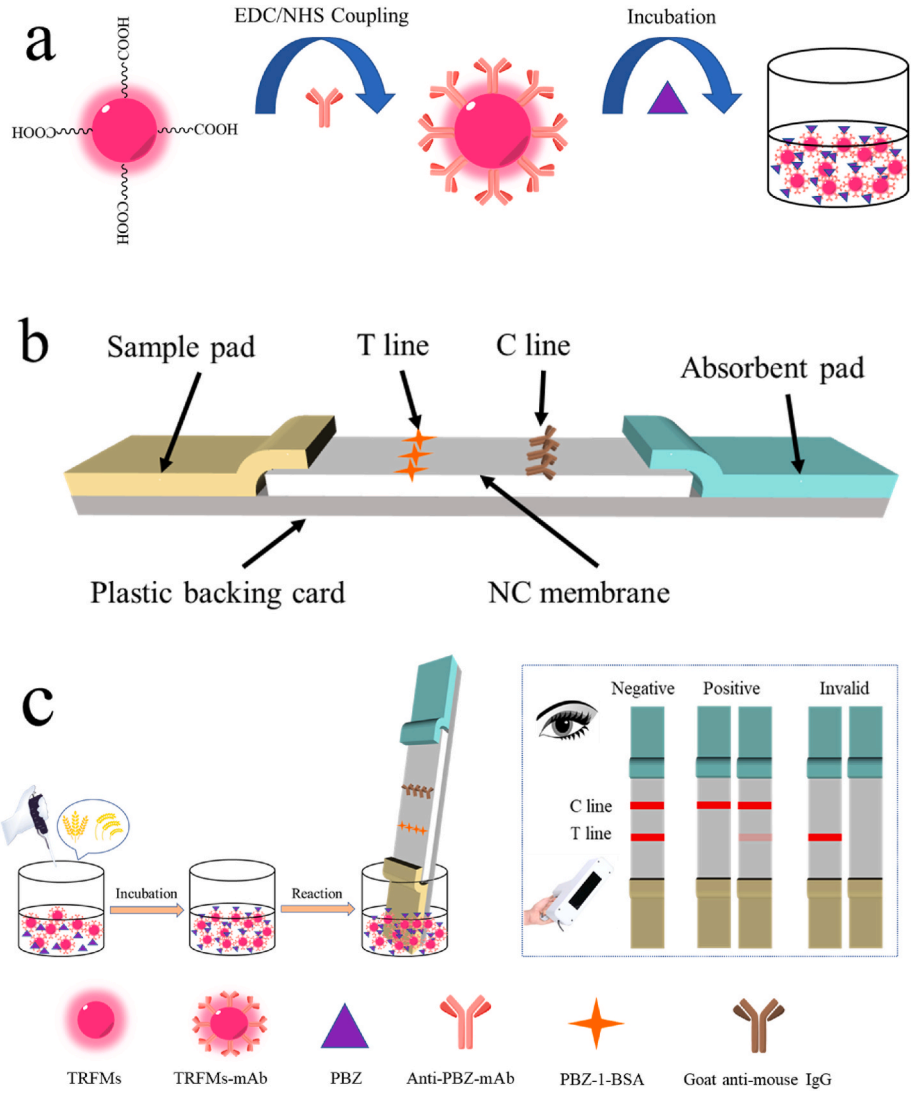

Fig. 1. The schematic of the TRFMs-LFIA strips for PBZ detection. a: the preparation principle of TRFMs immunoprobes; b: Components of LFIA strip; c: Schematic of PBZ detection by TRFMs-LFIA.

MAbs against PBZ (1 mg/mL) in optimized volume were added and stirred for 1 h at 25 °C. Next 50 μL of BSA solution (100 mg/mL) was added to block the unbound active sites. After centrifuged for 15 min at 12,000 rpm and 4 °C, the sediment was dissolved in 200 μL of resuspension buffer (0.5 M PB, pH 7.4) containing 0.1% (v/v) Tween-20, 5% (w/v) trehalose, 1% (w/v) BSA, and 0.03% (v/v) procline-300 and kept at 4 °C in darkness. The TRFMs immunoprobes was characterization by Zetasizer Nano ZS90.

2.6. Establishment of TRFMs-LFIA

The LFIA strip comprises the following parts: sample pad for absorbing sample solution, NC membrane for immobilizing Test line and Control line and performing chromatography, absorbent pad for absorbing at the terminal, and plastic card for backing behind (Fig. 1b).

Coating antigen and goat anti-mouse IgG antibody (secondary antibody) were diluted to 2 mg/mL and 0.16 mg/mL respectively with coating buffer (20 mM PB with 0.15 M NaCl, pH 7.4), and then sprayed on the NC membrane as Test line and Control line, respectively. The spray volume was 0.7 μL/cm, then the membrane was desiccated at 37 °C in an oven. Next the sample pad was immersed in a pretreatment buffer (50 mM PB with 0.5% (v/v) Tween-20, 0.5% (w/v) BSA, 5% (w/v) sugar, and 5% (w/v) PVP, pH 7.4) for 1 h, and dried in an oven at 37 °C. Finally, the processed sample pad and NC membrane, together with the absorbent pad, were integrated on the backing pad in turn, and cut into 4 mm-wide strips and packaged in sealed bags for further use.

In this study, the strip adopted the competitive reaction mode (Fig. 1c). Optimized amount of TRFMs immunoprobes and 100 μL standard or sample extracts were incubated in the microplates for 3 min. Subsequently, the strip was vertically dipped in the microplate for 3 min. The test strips were visually inspected under UV light for qualitative results, and the fluorescence intensity of the T and C line were quantified by a FIC-Q1 multifunctional fluorescence reader for quantitative analysis. The concentrations of PBZ in the samples were calculated using the calibration curve.

2.7. Optimization of TRFMs-LFIA and assay evaluation

In order to achieve the ideal fluorescence intensity and improve the sensitivity of the assay, four conditions namely the activated pH, the mAbs diluent, the mAb reacting concentration, and the probe amount were optimized: 1. TRFMs immunoprobes were activated in MES buffer at pH 5.0, 5.5, 6.0 and 6.5; 2. 0.05 M PB (pH 7.4), 0.01 M PB (pH 7.4), 0.01 M PB (0.5% (w/v) BSA, pH 7.4), H_2O (0.5% (w/v) BSA), 0.002 M BB (pH 8.0) and H_2O were chosen as the mAbs diluents to prepare TRAMs immunoprobes; 3. TRAMs immunoprobes were prepared with different volume of 1 mg/mL mAb (0.5 μL, 1 μL, 1.5 μL, 2 μL); 4. Different volume of 7.5 μg/mL probe (2 μL, 3 μL, 4 μL, 5 μL) were added to the microwell for reaction. The optimal conditions were determined according to the fluorescence intensity, the inhibition rate and the intensity of background fluorescence on NC membrane of the test strip.

The assay sensitivity was evaluated by determining the visual limit of detection (vLOD), the standard curve, and quantitative limit of detection (qLOD). The vLOD was defined as the lowest PBZ level at which the T line could disappear. The standard curve was drawn taking the B/B_0 value as the Y-axis, and the logarithm of analyte levels as the X-axis, in which B and B_0 are the ratios of T fluorescence intensity to C fluorescence intensity with and without standard PBZ. The IC_{50} value is the PBZ concentration at 50% of antibody-antigen binding response. The qLOD were taken as the level corresponding to 80% B/B_0 calculated from the standard curves (Song et al., 2014; Zhang et al., 2017).

The specificity was determined by evaluating the cross reactivity (CR) of the anti-PBZ mAb with other structural analogues. It was calculated as follows (Xiao et al., 2018), CR (%) = IC_{50} (PBZ, ng/mL)/IC_{50} (structural analogue, ng/mL) × 100.

The TRFMs-LFIA strip and immunoprobes were placed at 37 °C for 1, 8, 16, and 30 d, and the stability of the TRFMs-LFIA was accessed by the change of the fluorescence signal intensity and inhibiting rate to 40 ng/mL of PBZ.

2.8. Recovery test and real sample analysis

Rice and wheat purchased from local markets were detected by UPLC-MS/MS and identified to be PBZ-free. All samples were ground into powder and sieved through 100 mesh. Rice and wheat powder (5 g) were weighed and distributed in 10 mL PB (0.1 M, pH 7.4) containing 40% methanol, then vortexed for 15 min and centrifugated at 4500 rpm for 15 min at room temperature. The sample extracts were collected for further analysis.

Matrix effect was eliminated by gradient dilution method. Negative sample was pretreated according to the above steps, next the supernatant was diluted by PB and tested with TRFMs-LFIA strips. The dilution multiple in which fluorescence intensity is close to that in original PB buffer is chosen for the elimination of sample matrix.

For validation of accuracy, rice and wheat samples spiked with three levels of PBZ were detected via TRFMs-LFIA and UPLC-MS/MS in triplicates. 10 rice and 10 wheat real samples were pretreated and detected by TRFMs-LFIA strips, followed by UPLC-MS/MS verification. The UPLC-MS/MS was performed using the mode of multiple reaction monitoring (MRM) through an electrospray ionizaction (ESI) positive-ion source. The extract supernatant samples were analyzed on BEH C_{18} column (50 mm × 2.1 mm, 1.7 μm) and the temperature was 40 °C. The mobile phase was acetonitrile (A) and ultrapure water (B). The gradient elution procedure was programmed as follows: 0–0.5 min, 100%–90% B; 0.5–2 min, 90% B–50% B; 2–5 min, 50% B–35% B; 5–8 min, 35%–0% B; 8–9 min, 0% B, 9–9.1 min, 0% B–90% B. The injection volume and flow rate were 0.1 μL and 0.3 mL/min, respectively.

3. Results and discussion

3.1. Synthesis of antigens

Haptens designing and synthesizing are the prerequisites and key steps for successful preparation of mAb. Two PBZ haptens were synthesized and identified by LC-MS and NMR, and the results are as follow:

PBZ-1: ESI-MS, m/z 393.9 ([M+H]+).^{1}H NMR (600 MHz, CD_3OD): δ 8.64 (s, 12H), 7.83 (s, 12H), 7.16 (d, J = 8.5 Hz, 24H), 7.06 (d, J = 8.5 Hz, 25H), 5.17 (s, 13H), 3.31 (s, 23H), 2.57 (s, 71H), 0.77 (s, 110H). ^{13}C NMR (151 MHz, CD_3OD): δ 176.08 (d, J = 6.1 Hz), 174.02, 150.69, 145.42, 136.78, 133.74, 131.66, 129.43, 80.28, 63.61, 49.00, 40.07, 36.01, 30.22, 29.85, 26.28.

PBZ-2: ESI-MS, m/z 428 ([M-H]-).^{1}H NMR (600 MHz, $CDCl_3$): δ 8.51 (s, 8H), 8.13 (d, J = 8.4 Hz, 16H), 7.85 (s, 8H), 7.44 (d, J = 8.4 Hz, 16H), 7.26 (s, 4H), 7.21 (d, J = 8.5 Hz, 16H), 6.95 (d, J = 8.5 Hz, 16H), 4.86 (d, J = 11.5 Hz, 16H), 4.71 (d, J = 11.5 Hz, 8H), 3.45 (d, J = 2.8 Hz, 8H), 3.29 (d, J = 9.8 Hz, 7H), 3.20 (s, 6H), 0.89 (s, 72H). ^{13}C NMR (151 MHz, $CDCl_3$): δ 169.49, 149.44, 144.40,143.07 135.16, 133.19,130.57, 130.05, 129.11,126.95, 87.48, 77.16,76.41, 63.84, 40.60,36.69, 26.72, 1.16.

Because the molecular weight of PBZ was too small to have immunogenicity, a complete antigen was formed by chemically linking PBZ to a larger immunogenic carrier protein (OVA/BSA/KLH/THY). The complete antigens were characterized by the UV–Vis spectra. The hapten and carrier protein have different characteristic absorption peaks. Therefore, after successful coupling of hapten and carrier protein, the conjugate should have characteristic absorption peaks of both hapten and carrier protein, or due to structural changes, the characteristic absorption peaks of artificial antigen will be shifted relative to the original carrier protein (Kong et al., 2010). As shown in Fig. S2, carrier proteins generally have absorption peaks around 280 nm, and haptens PBZ-1 and PBZ-2 have characteristic absorption peaks at around 320 nm, while the characteristic absorption peaks of complete antigens are shifted compared to

those of the haptens and carrier proteins, which can preliminarily prove that the complete antigens were synthetized successfully.

3.2. Preparation and characterization of anti-PBZ mAb

The icELISA results of antisera test showed (Table 2) that the mice immunized by three kinds of immunogen all have the immunogenic effect, and the detection sensitivity could be significantly improved by using PBZ-2-BSA as a heterogeneous coating antigen. This could be because the affinity between antibody and heterologous coating antigen is lower than that of antibody with homologous coating antigen, and the former results in stronger binding of PBZ to antibody (Chen et al., 2017). Furthermore, compared with other two immunogens, PBZ-1-THY has the best immunogenic effect, which exhibiting the highest titer and inhibition rate (1:16000, 89%). Therefore, all subsequent experiments were performed with PBZ-1-THY as the immunogen and PBZ-2-BSA as the coating antigen.

After cell fusion and four rounds of sub-cloning, the hybridoma cell line 1C1 showed the highest sensitivity against PBZ. So 1C1 was selected to produce the mAb. After purified by protein G affinity chromatography, the mAb was concentrated to 11.03 mg/mL. The purity of antibody was verified by SDS-PAGE gel electrophoresis. As shown in Fig. S3, under the reduction condition, the disulfide bond connecting the antibody was broken when the antibody was heated, forming a heavy chain band of about 50 kDa and a light chain band of about 25 kDa. Under non-reduction conditions, the molecular weight of mAb is about 150 kDa, so the antibody only displayed a band of about 150 kDa. Thus, it can be proved that the mAb was in high purity. The subtype of the mAb was identified as IgG1 (Fig. S4), and the IC_{50} of it detected by icELISA was 3.72 ng/mL (Fig. S5).

3.3. Characterization of the TRFMs immunoprobes

In order to obtain uniform and stable TRFMs immunoprobes, the microspheres should have uniform particle size, uniform dispersity, and smooth spherical edges (Li et al., 2021). Characterization of the shape and size of the TRFMs were performed by TEM (Fig. 2a) and Zetasizer Nano ZS90 (Fig. 2b). TRFMs was monodisperse spherical particles with complete structure, uniform size and the mean diameter was about 200 nm, which can be used for the subsequent development of TRFMs-LFIA. It was found that there are obvious changes in particle size and zeta potential after the synthesis of TRFMs-antibody conjugate (Chen et al., 2022). As presented in Fig. 2c and Fig. 2d, the Zeta potential of TRFMs changed significantly from −43.8 mV to −22.7 mV, and the average particle size increased from 204.9 nm to 299.9 nm after the addition of mAbs. These results confirmed that the antibody was immobilized on the fluorescence microspheres to form TRFMs immunoprobes.

3.4. Optimization of the TRFMs-LFIA

The probe was prepared by active ester method, and TRFMs was conjugated to the antibody through carboxyl groups. The pH value will affect the coupling efficiency and even cause coagulation of the conjugate (Wang et al., 2020). From the results (Fig. 3a), we found that when the pH was 5.0, both the T line and the C line were difficult to develop color due to the antibody precipitation. When the pH was 6.0, the fluorescence intensity of the strip was ideal, and the inhibiting rate was also the highest. Therefore, we chose pH 6.0 as the optimal pH value for activation buffer.

In order to improve coupling efficiency and reduce non-specific adsorption, six different antibody diluents were used to dilute antibody. The results were shown in Fig. 3b. The two diluents containing BSA got the lowest inhibition rate. This is probably because BSA will bind to the antibody first and play a blocking role, resulting in a lower coupling rate between the TRFMs and the antibody, thereby affecting the fluorescence intensity and inhibition rate (Liu et al., 2020). In addition, the proper ion concentration also helps to maintain protein activity (Chen et al., 2022). As shown in Fig. 3b, 0.05 M PB (pH 7.4) exhibited the best inhibitory effect and achieved the required fluorescence intensity. Thus, it was selected as the mAbs dilution buffer.

Appropriate amount of antibody will get a good color rendering effect, and reduce steric hindrance to improve coupling efficiency (Wu et al., 2021; Li et al., 2021). From the results shown in Fig. 3c, as the amount of antibody increasing, the fluorescence intensity increased gradually. While the amount of antibody was greater than 1.5 μL (1.5 μg), the inhibition effect became significantly worse, which indicating that the binding of antibody and microspheres has reached saturation. Therefore, 1.5 μL (1.5 μg) was selected as the optimal amount of antibody.

The amount of probe was also a key factor which will affect the color development and inhibitory effect of the strip. An excessive amount will cause background fluorescence interference (Liu et al., 2022). As shown in Fig. 3d, 2–5 μL of probe (7.5 μg/mL) was selected for optimization. As the probe amount increasing, the fluorescence intensity was also enhanced, but resulting in the decreased inhibition rate from 3 μL. Meanwhile, when the volume of probe reached to 5 μL, significant background fluorescence interference occurred. Thus, 3 μL probe with ideal fluorescence intensity and inhibition rate was chosen for the following study.

3.5. Assay evaluation

Under the optimal conditions, the sensitivity of TRFMs-LFIA was tested by a series of PBZ levels (0, 1.56, 3.12, 6.25, 12.5, 25, 50 and 100 ng/mL). As show in Fig. 4, the vLOD of the TRFMs-LFIA was 50 ng/mL, the qLOD and the IC_{50} of the assay were 1.72 and 9.38 ng/mL, which was below the MRL of China (GB 2763-2021). The detection time of the proposed TRFMs-LFIA in this research was 6 min. The sensitivity of the developed TRFMs-LFIA for PBZ was comparable to the previously reported icELISA, and more importantly, the detection speed was 10 folds faster than them (Wang, 2016; Ouyang et al., 2020; Jin, 2019).

Stability plays a key role in a developed method. The stability test results (Fig. 5) showed that the fluorescence intensity and inhibiting rate did not decrease significantly after been placed at 37 °C for 30 d, which could prove good stability of the established TRFMs-LFIA.

The CR of PBZ with other structural analogues was also evaluated. The results in Table 3 revealed that the TRFMs-LFIA exhibited slight CR towards triadimefon (2.1%), triadimenol (1.01%), uniconazole (0.25%) and negligible CR (<0.1%) with the other three structural analogues. This suggested that the proposed TRFMs-LFIA preformed highly specific to PBZ.

3.6. Recovery test and real sample analysis

When the rice and wheat extracts were diluted 2- and 8-fold respectively, the influence of matrix effect was basically eliminated (Fig. S6). Therefore, the sample extracts of rice and wheat were diluted by 2-fold and 8-fold respectively before tested by TRFMs-LFIA.

Table 4 showed that the average recoveries ranged from 96.2% to 111.9% with CV of 4.0%–11.2% for TRFMs-LFIA. Good correlation was observed between TRFMs-LFIA and UPLC-MS/MS ($y = 0.934x + 0.143$,

Table 2
Characterization of mouse antisera against PBZ.

Immunogen	Coating antigen	Titer	Inhibition rate (%)
PBZ-1-OVA	PBZ-1-BSA	1:8000	27
PBZ-1-KLH		1:16000	20
PBZ-1-THY		1:16000	23
PBZ-1-OVA	PBZ-2-BSA	1:16000	77
PBZ-1-KLH		1:16000	83
PBZ-1-THY		1:16000	89

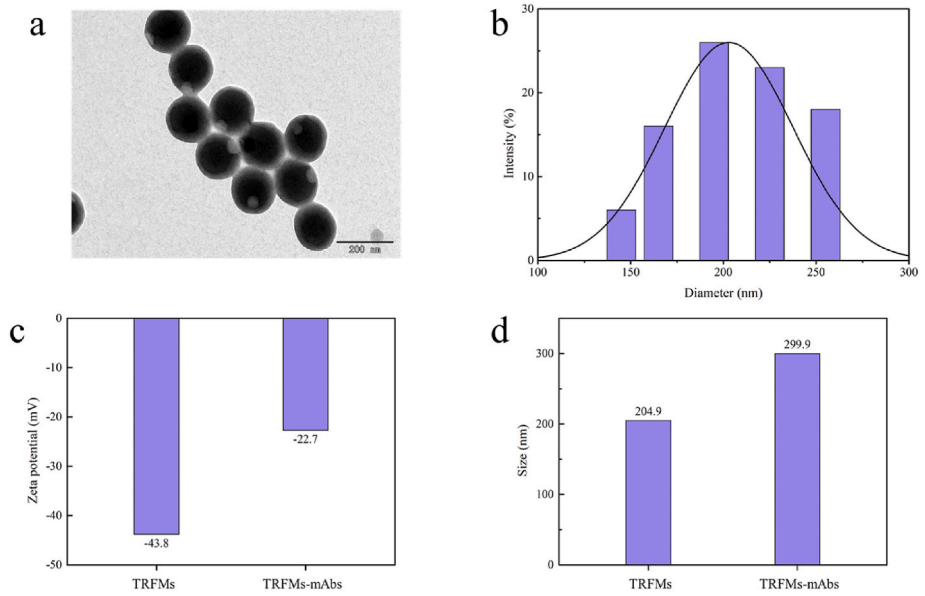

Fig. 2. Characterization of the TRFMs and TRFMs-mAbs probe. a: TEM image of TRFMs; b: particle size distribution of TRFMs; c: Zeta potential of TRFMs and TRFMs-mAbs probe. d: particle size of TRFMs and TRFMs-mAbs probe.

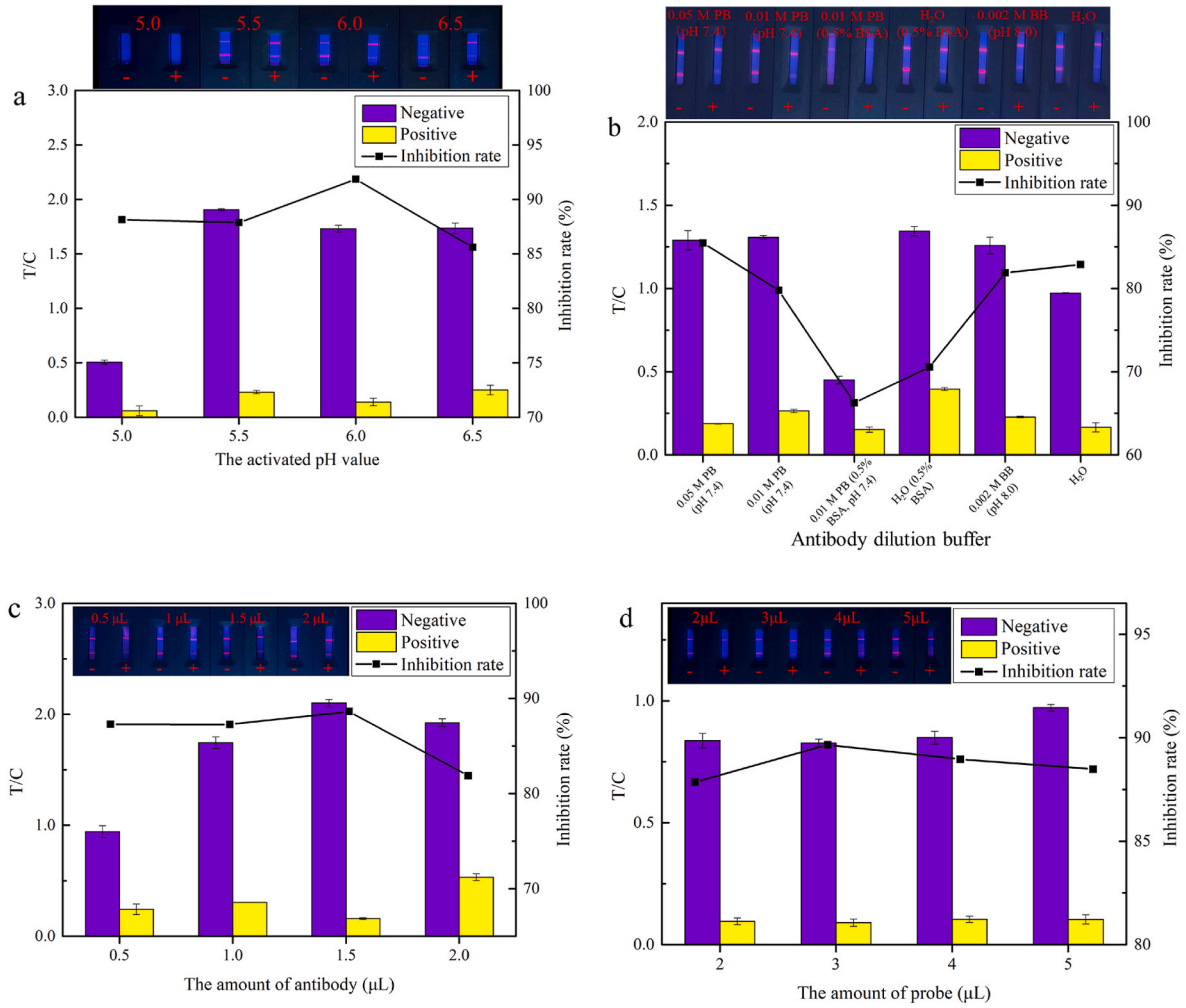

Fig. 3. Optimization of the TRFMs-LFIA (n = 3). a: the activated pH value; b: the mAbs dilution buffer; c: the amount of antibody (μL in 1 mg/mL); d: the amount of probe (μL in 7.5 μg/mL).

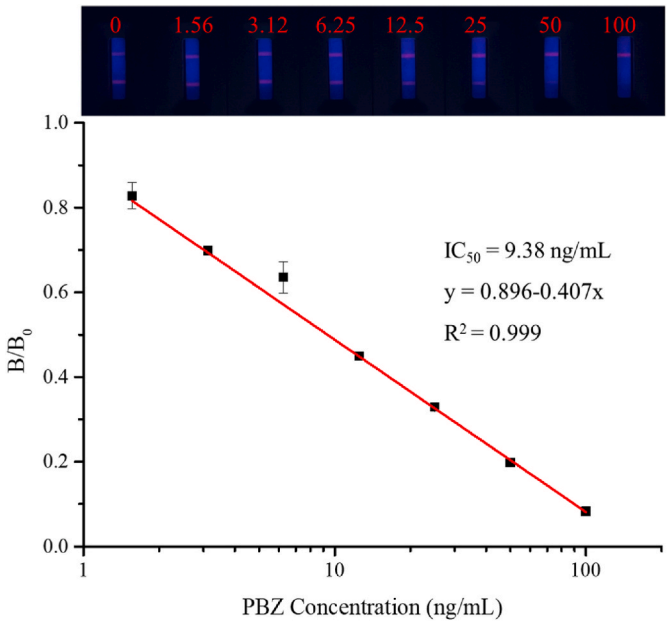

Fig. 4. Calibration curve for PBZ detection by TRFMs-LFIA (n = 3).

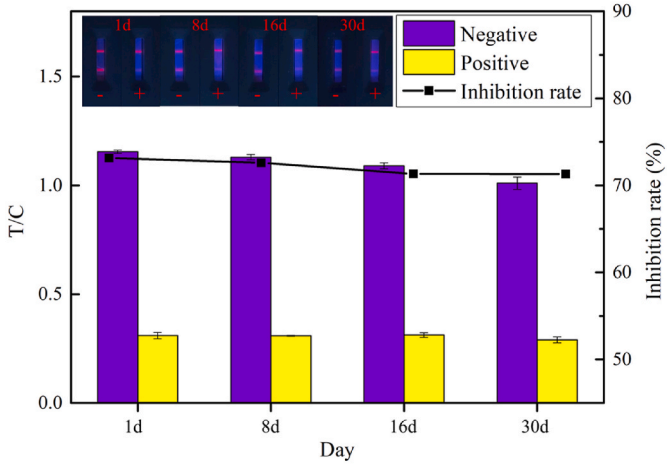

Fig. 5. Stability of the TRFMs-LFIA(n = 3).

$R^2 = 0.99$) (Fig. S7). Besides, three kinds of blind samples including rice (n = 10), wheat (n = 10), and pakchoi (n = 6) were also analyzed with TRFMs-LFIA and UPLC-MS/MS simultaneously. As shown in Table S1, the results of TRFMs-LFIA were correlated well with that of UPLC-MS/MS. These results indicate that the TRFMs-LFIA was accurate and reliable for all tested samples, and it can be adopted for analyzing PBZ rapidly and effectively in real samples.

4. Conclusion

In this study, a TRFMs-LFIA was established using an anti-PBZ mAb to detect PBZ residues in cereals. First, two haptens were synthesized and conjugated to carrier proteins to prepare artificial antigens, and a sensitive anti-PBZ mAb was prepared. Then, the PBZ mAb was combined with Eu^{3+} doped TRFMs to develop an on-site lateral flow immunoassay that can qualitatively or quantitatively detect PBZ residues within 6 min. After optimization, the qLOD and IC_{50} of the proposed assay were 1.72 and 9.38 ng/mL, respectively. The developed TRFMs-LFIA method has good specificity to PBZ, and the CR with six structural analogues were all below 3%. The recovery rate of PBZ in spiked rice and wheat samples was 96.2%–111.9% with CV of 4.0%–11.2%, indicating that the developed TRFMs-LFIA is accurate and precise. The blind samples detecting results show that the proposed method is consistent with UPLC-MS/MS. The proposed LFIA demonstrated a comparable accuracy and specificity with previously reported immunoassays [TRFIA (Liu et al., 2016) and ELISA (Cao et al., 2014; Ouyang et al., 2020)], but it is faster, simpler, more economical and convenient compared with them. Overall, in this research, the TRFMs-LFIA provides a novel and credible analytical assay for rapid on-site PBZ detecting.

Table 3
Cross-reactivity (CR) of PBZ with structural analogues.

Analytes	Structure	IC_{50} (ng/mL)	CR (%)
Paclobutrazol	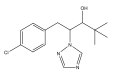	9.35	100
Tebuconazole	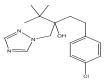	>10000	<0.1
Triadimefon	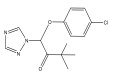	443.71	2.10
Hexaconazole	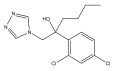	>10000	<0.1
Diniconazole	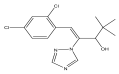	>10000	<0.1
Triadimenol	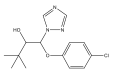	924.21	1.01
Uniconazole	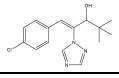	3815.16	0.25

Table 4
Results of recovery test of PBZ in rice and wheat samples by TRFMs-LFIA (n = 3).

Samples	Spiked level (ng/g)	Level in sample solution (ng/mL)	TRFMs-LFIA results		
			Mean ± SD (ng/mL)	Recovery (%)	CV (%)
Rice	16	4	3.8 ± 0.4	96.2	11.2
	32	8	7.8 ± 0.8	97.9	10.9
	160	40	39.8 ± 0.5	98.3	6.7
Wheat	64	4	4.4 ± 0.3	111.9	8.0
	128	8	8.4 ± 0.3	105.1	4.0
	640	40	43.7 ± 0.5	109.2	9.1

Funding

This work was supported by the Guangdong Basic and Applied Basic Research Foundation (2019A1515012107).

Institutional review board statement

All procedures involving animals were performed in accordance with the protective and administrant laws for laboratory animals of China and approved by the Institutional Authority for Laboratory Animal Care.

CRediT authorship contribution statement

Yongjian Cheng: Methodology, Visualization, Writing – original draft. **Bo Xie:** Formal analysis, Validation. **Yifan Liang:** Validation. **Xinmei Liu:** Validation. **Haojie Chen:** Validation. **Jiadong Li:** Validation. **Hongtao Lei:** Writing – review & editing. **Zhili Xiao:** Conceptualization, Supervision, Writing – review & editing, Funding acquisition.

Declaration of competing interest

The authors declare that they have no known competing financial interests or personal relationships that could have appeared to influence the work reported in this paper.

Appendix A. Supplementary data

Supplementary data to this article can be found online at https://doi.org/10.1016/j.crfs.2022.08.017.

References

Authority, E.F.S., 2007. Reasoned opinion on the potential chronic and acute risk to consumers health arising from proposed temporary EU MRLs. EFSA J. https://doi.org/10.2903/j.efsa.2007.32r.

Cao, Z., Zhao, H., Cui, Y., et al., 2014. Development of a sensitive monoclonal antibody-based enzyme-linked immunosorbent assay for the analysis of paclobutrazol residue in wheat Kernel. J. Agric. Food Chem. 62 (8), 1826–1831. https://doi.org/10.1021/jf404905w.

Chen, Z., Fu, H., Luo, L., Sun, Y., Yang, J., Zeng, D., Shen, Y., Xu, Z., 2017. Development of competitive indirect ELISAs with a flexible working range for the simple quantification of melatonin in medicinal foods. Anal. Methods 9 (10). https://doi.org/10.1039/C6AY03380F.

Chen, B., Shen, X., Lei, H., et al., 2022. Antibody generation and rapid immunochromatography using time-resolved fluorescence microspheres for propiconazole: fungicide abused as growth regulator in vegetable. Foods 11 (3). https://doi.org/10.3390/foods11030324.

Cregg, B., Ellison-Smith, D., 2020. Application of paclobutrazol to mitigate environmental stress of urban street trees. Forests 11 (3), 355. https://doi.org/10.3390/f11030355.

Galfre, G., Milstein, C., 1981. Preparation of monoclonal antibodies: strategies and procedures. Clin. Vacc. Immunol. CVI 73 (2), 3–46. https://doi.org/10.1016/0076-6879(81)73054-4.

B 2763-2021, National food safety standard—Maximum residue limits for pesticides in food [S].

Gonçalves, I.C.R., Araújo, A.S.F., Carvalho, E.M.S., et al., 2009. Effect of paclobutrazol on microbial biomass, respiration and cellulose decomposition in soil. Eur. J. Soil Biol. 45 (3), 235–238. https://doi.org/10.1016/j.ejsobi.2009.01.002.

Guo, H., Zhao, Y., Ouyang, M., et al., 2021. Different degradation patterns of chiral contaminant enantiomers: paclobutrazol as a case study. J. Braz. Chem. Soc. https://doi.org/10.21577/0103-5053.20210001.

Hua, S., Zhang, Y., Yu, H., et al., 2014. Paclobutrazol application effects on plant height, seed yield and carbohydrate metabolism in canola. Int. J. Agric. Biol. 16 (3) https://doi.org/10.1590/brag.2014.011.

Jiang, X., Wang, Y., Xie, H., et al., 2019. Environmental behavior of paclobutrazol in soil and its toxicity on potato and taro plants. Environ. Sci. Pollut. Control Ser. 26 (26), 27385–27395. https://doi.org/10.1007/s11356-019-05947-9.

Jin, X., 2019. Establishment of a Rapid Detection Method for Paclobutrazol and the Effect of Chiral Compounds on Soil Bacterial Diversity. Hainan university. https://doi.org/10.27073/d.cnki.ghadu.2019.000632.

Juntunen, E., Myyryläinen, T., Salminen, T., et al., 2012. Performance of fluorescent europium (III) nanoparticles and colloidal gold reporters in lateral flow bioaffinity assay. Anal. Biochem. 428 (1), 31–38. https://doi.org/10.1016/j.ab.2012.06.005.

Kishore, K., Singh, H.S., Kurian, R.M., 2015. Paclobutrazol use in perennial fruit crops and its residual effects: a review. Indian J. Agric. Sci. 85 (7), 863–872.

Kokko, L., Lövgren, T., Soukka, T., 2007. Europium (III)-chelates embedded in nanoparticles are protected from interfering compounds present in assay media. Anal. Chim. Acta 585 (1), 17–23. https://doi.org/10.1016/j.aca.2006.12.006.

Kong, T., Liu, G., Li, X., Wang, Z., Zhang, Z., Xie, G., Zhang, Y., Sun, J., Xu, C., 2010. Synthesis and identification of artificial antigens for cadmium and copper. Food Chem. 123 (4) https://doi.org/10.1016/j.foodchem.2010.05.087.

Anfossi, Laura, Claudio, Baggiani, Cristina, Giovannoli, Gilda, D'Arco, Gianfranco, Giraudi, 2013. Lateral-flow immunoassays for mycotoxins and phycotoxins: a review. Anal. Bioanal. Chem. 405 (2-3) https://doi.org/10.1007/s00216-012-6033-4.

Li, M., Wang, H., Sun, J., et al., 2021. Rapid, on-site, and sensitive detection of aflatoxin M1 in milk products by using time-resolved fluorescence microsphere test strip. Food Control 121, 107616. https://doi.org/10.1016/j.foodcont.2020.107616.

Li, X., Chen, X., Wu, J., et al., 2021. Portable, rapid, and sensitive time-resolved fluorescence immunochromatography for on-site detection of dexamethasone in milk and pork. Foods 10 (6), 1339. https://doi.org/10.3390/foods10061339.

Liu, C., Ma, W., Gao, Z., Huang, J., Hou, Y., Xu, C., Yang, W., Gao, M., 2014. Upconversion luminescence nanoparticles-based lateral flow immunochromatographic assay for cephalexin detection. J. Mater. Chem. C 2 (45). https://doi.org/10.1039/C4TC02034K.

Liu, H., Lin, T., Mao, J., et al., 2015. Paclobutrazol residue determination in potato and soil using low temperature partition extraction and ultrahigh performance liquid chromatography tandem mass spectrometry. J. Anal. Methods Chem. 2015, 1–6. https://doi.org/10.1155/2015/404925.

Liu, Y., Wu, A., Hu, J., Liu, X., 2015. Detection of 3-phenoxybenzoic acid in river water with a colloidal gold-based lateral flow immunoassay. Anal. Biochem. 483 https://doi.org/10.1016/j.ab.2015.04.022.

Liu, Z., Wei, X., Ren, K., et al., 2016. Highly efficient detection of paclobutrazol in environmental water and soil samples by time-resolved fluoroimmunoassay. Sci. Total Environ. 569–570, 1629–1634. https://doi.org/10.1016/j.scitotenv.2016.06.089.

Liu, Z., Hua, Q., Li, X., et al., 2020. A smartphone-based dual detection mode device integrated with two lateral flow immunoassays for multiplex mycotoxins in cereals. Biosens. Bioelectron. 158 https://doi.org/10.1016/j.bios.2020.112178.

Liu, Z., Hua, Q., Wang, J., et al., 2022. Prussian blue immunochromatography with portable smartphone-based detection device for zearalenone in cereals. Food Chem. 369, 131008 https://doi.org/10.1016/j.foodchem.2021.131008.

Di Nardo, Fabio, Matteo, Chiarello, Cavalera Simone, Claudio, Baggiani, Laura, Anfossi, 2021. Ten years of lateral flow immunoassay technique applications: trends, challenges and future perspectives. Sensors 21 (15). https://doi.org/10.3390/s21155185.

Ouyang, Q., Liu, X., Tan, R., et al., 2020. Polyclonal antibody-based indirect competitive enzyme-linked immunosorbent assay for screening of paclobutrazol in fruits. J. Environ. Sci. Health Part B 55 (3), 250–256. https://doi.org/10.1080/03601234.2019.1685319.

Peng, D., Chen, X., Yin, Y., et al., 2014. Lodging resistance of winter wheat (Triticum aestivum L.): lignin accumulation and its related enzymes activities due to the application of paclobutrazol or gibberellin acid. Field Crop. Res. 157, 1–7. https://doi.org/10.1016/j.fcr.2013.11.015.

Posthuma-Trumpie Geertruida, A., Jakob, Korf, van Amerongen Aart, 2009. Lateral flow (immuno)assay: its strengths, weaknesses, opportunities and threats. A literature survey. Anal. Bioanal. Chem. 393 (2) https://doi.org/10.1007/s00216-008-2287-2.

Sancho, J.V., Pozo Ó, J., Zamora, T., et al., 2003. Direct determination of paclobutrazol residues in pear samples by liquid chromatography-electrospray tandem mass spectrometry. J. Agric. Food Chem. 51 (15), 4202–4206. https://doi.org/10.1021/jf034107s.

Mihaela, Savin, Carmen-Marinela, Mihailescu, Iulia, Matei, Dana, Stan, Carmen Aura, Moldovan, Ion, Marian, Baciu, Ion, 2018. A quantum dot-based lateral flow immunoassay for the sensitive detection of human heart fatty acid binding protein (hFABP) in human serum. Talanta 178. https://doi.org/10.1016/j.talanta.2017.10.045.

Shah, A.N., Tanveer, M., Rehman, A.U., et al., 2017. Lodging stress in cereal—effects and management: an overview. Environ. Sci. Pollut. Control Ser. 24 (6), 5222–5237. https://doi.org/10.1007/s11356-016-8237-1.

Shan, S., Lai, W., Xiong, Y., Wei, H., Xu, H., 2015. Novel strategies to enhance lateral flow immunoassay sensitivity for detecting foodborne pathogens. J. Agric. Food Chem. 63 (3) https://doi.org/10.1021/jf5046415.

Song, S., Liu, N., Zhao, Z., et al., 2014. Multiplex lateral flow immunoassay for mycotoxin determination. Anal. Chem. 86 (10), 4995–5001. https://doi.org/10.1021/ac500540z.

Sun, J., Wang, L., Shao, J., Yang, D., Fu, X., Sun, X., 2021. One-step time-resolved fluorescence microsphere immunochromatographic test strip for quantitative and simultaneous detection of DON and ZEN. Anal. Bioanal. Chem. 413 (26) https://doi.org/10.1007/s00216-021-03612-0.

Wang, M., 2016. Fundamental Study on Immunoassays for the Determination of Salbutamol and Paclobutrazol. Jiangsu University. https://doi.org/10.7666/d.D01001884.

Wang, X., Wu, X., Lu, Z., et al., 2020. Comparative study of time-resolved fluorescent nanobeads, quantum dot nanobeads and quantum dots as labels in fluorescence immunochromatography for detection of aflatoxin B_1 in grains. Biomolecules 10 (4), 575. https://doi.org/10.3390/biom10040575.

Wu, S., Miao, Y., Hu, Z., et al., 2015. Enantioselective degradation of (2RS, 3RS)-paclobutrazol in rat liver microsomes. Chirality 27 (5). https://doi.org/10.1002/chir.22440.

Wu, Q., Yao, L., Qin, P., et al., 2021. Time-resolved fluorescent lateral flow strip for easy and rapid quality control of edible oil. Food Chem. 357, 129739 https://doi.org/10.1016/j.foodchem.2021.129739.

Xiao, Z., Wang, Y., Shen, Y., et al., 2018. Specific monoclonal antibody-based enzyme immunoassay for sensitive and reliable detection of alternaria mycotoxin iso-tenuazonic acid in food products. Food Anal. Methods. https://doi.org/10.1007/s12161-017-1033-9.

Xu, Q., Xu, H., Gu, H., Li, J., Wang, Y., Wei, M., 2009. Development of lateral flow immunoassay system based on superparamagnetic nanobeads as labels for rapid quantitative detection of cardiac troponin I. Mater. Sci. Eng. C 29 (3). https://doi.org/10.1016/j.msec.2009.01.009.

Zhang, X., Yu, X., Wen, K., et al., 2017. Multiplex lateral flow immunoassays based on amorphous carbon nanoparticles for detecting three Fusarium mycotoxins in maize. J. Agric. Food Chem. 65 (36), 8063–8071. https://doi.org/10.1021/acs.jafc.7b02827.